How does vestibule surface charge affect ion conduction and toxin binding in a sodium channel?

Mao Cai and Peter C. Jordan
Department of Chemistry, Brandeis University, Waltham, Massachusetts 02254

ABSTRACT We describe various models for the dielectric geometry and pore mouth charge distribution of a Na channel. The electric potential due to the vestibule charges is then computed on the basis of the nonlinear Possion-Boltzmann equation. The results are used to account for the effect of permeant ion concentration and ionic strength on channel conductance and on toxin association rate constants for Na channels. We find that a single negatively charged group near the entrance to the channel constriction is adequate to account for deviations from Michaelis-Menten conductance kinetics and for the concentration dependence of toxin-binding coefficients. We find further that only a limited range of vestibule geometries and pore mouth charge distributions are consistent with experiment.

INTRODUCTION

It has long been recognized that electrostatic interactions play important roles in controlling the transport of permeant ions and the binding of toxins and other blockers in membrane-channel systems (for recent reviews see Jordan, 1986; Miller and Garber, 1988). These interactions are of three main types. First, as an ion approaches the channel mouth from solution, the membrane is polarized because the membrane and the solution provide different dielectric environments; thus ions experience a repulsive force due to the image charges induced in the membrane. Second, if the channel forming protein has charged or polar groups, they interact with ions and thereby affect ionic access to and transport across the channel. Third, if the membrane is itself charged, it too can influence the electrical potential along the conductance pathway and, thereby, the channel conductance. Image forces in channels have been exhaustively studied. In addition to their direct influence on permeation in singly occupied channels (Parsegian, 1969; Levitt, 1978; Jordan, 1982), they are believed to have an important influence on multiple occupancy (Hille and Schwartz, 1978; Hess and Tsien, 1984; Jordan, 1984, 1986). The electrostatic consequences of protein charge distributions and membrane surface charges have not been as carefully investigated for channel systems.

The main difficulty in assessing the electrostatic influence of local and membrane charge distributions on channel conductance is that little detailed information is available about the structure, composition, and electrical charge distribution in physiological channel environments. However, even if such information were available, the computational question is a complex one. Exact solutions for specific model channel geometries and charge distributions have been presented for systems at zero ionic strength (no electrolyte present) (Jordan, 1983, 1986, 1987). In the presence of electrolyte, the problem is greatly complicated because solutions to the nonlinear Poisson-Boltzmann equations are needed to obtain realistic estimates of the electric potential (Dani, 1986). In Na channels there is substantial evidence for the presence of negatively charged vestibules. These attract Na^+ ions, increasing the local vestibule concentration above its bulk value. Consequently conductance and blocking data do not appear to follow a simple Michaelis-Menten formalism. To account for the deviations, previous attempts to correlate conductance data and toxin binding data for the Na channel (Green et al., 1987*a* and *b*; Ravindran and Moczydlowski, 1989) have been based upon a simplified and unrealistic model, Gouy-Chapman (GC) theory. The GC picture, presuming an infinite plane of surface charge at the membrane water interface, is useful, although not truly reliable, for considering the influence of membrane charges. However, for the question of how fixed and finite protein charge distributions affect conductance, it is not only too simple but also inappropriate. Because the plane of charge is infinite, the model has as one of its basic consequences the prediction that, for charged surfaces and as permeant ion concentration decreases, channel conductance should approach a constant limit, even if permeant ion concentration approaches zero. Naturally all investigators applying GC theory as a tool to account for the influence that infinite vestibule surface charges have on conductance are fully aware of this difficulty. However, in the presence of a

0006-3496/90/04/883/09 $2.00

more reasonable model, GC theory has been the method of convenience. A new model is needed to better describe electrostatic interaction between the mobile ions and the fixed charge distributions of the protein.

In this paper a more realistic model for the dielectric geometry and pore mouth charge distribution in the Na channel is described. It is effectively an elaboration of GC theory to more general geometries and charge distributions. The electric potential in the channel vestibule is then computed on the basis of the nonlinear Poisson-Boltzmann equation. The results provide a basis by which to interpret recent conductance and toxin binding measurements on Na channels. We find the data can only be correlated on the basis of a rather limited set of structural models.

THEORY

The geometrical model we propose for the Na channel is illustrated in Fig. 1. It is cylindrically symmetric and possesses a funnel shape, a narrow tunnel with a gradually widening mouth. This structure is consistent with recent speculations (Begenisich, 1987) and analogous to that of the AChR channel which has a geometry similar to that illustrated (Kistler et al., 1982). As in real Na channels,

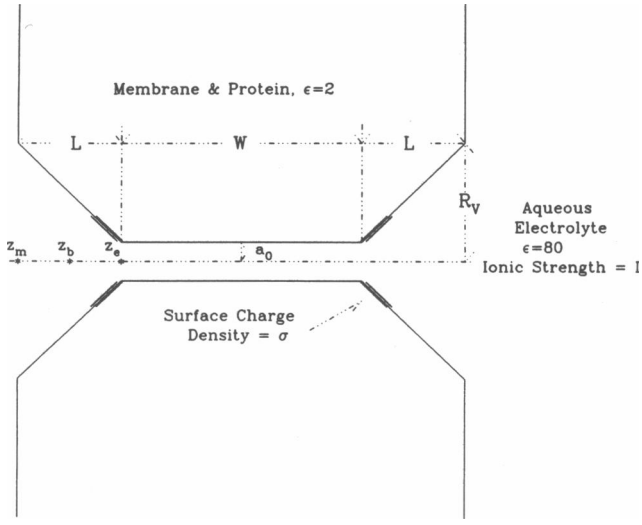

FIGURE 1 Geometry of the cylindrically symmetric model Na channel and electrolyte system. The regions to the right and left of the membrane contain aqueous electrolyte. The ionic strength I and the dielectric constant ϵ for the funnel-shaped channel can be varied to suit the physiological model of interest. In our calculation, it is assumed that I and ϵ for the mouth are the same as the bulk solution, while I for the narrow pore is zero and ϵ is same as the bulk water. The dotted regions near the constriction entrance indicate the location of vestibule charges.

the left- and right-hand side need not be symmetric. Cylindrically symmetric electrical sources are placed near the mouth. The channel and the membrane are immersed in aqueous solutions which contain electrolytes. The dielectric constant ϵ of the aqueous solution is 80 and that of membrane and protein are 2. For the narrow pore, the dielectric constant ϵ can be varied depending on the diameter of the pore. If the pore is wide enough, the water structure is essentially that of bulk water and ϵ is 80. If the pore is narrow, water is aligned in a wholly different way and ϵ is unknown, quite possibly significantly reduced.

The electric potential at every point is satisfied by the Poisson equation:

$$\nabla \cdot [\epsilon(r)\nabla\phi(r)] + 4\pi\rho_B(r) + 4\pi\rho_0(r) = 0, \quad (1)$$

where $\epsilon(r)$ is the local dielectric constant, $\rho_B(r)$ and $\rho_0(r)$ are the charge densities due to electrolytes and fixed electric sources, respectively, and $\phi(r)$ is the local potential. At equilibrium and at sufficiently low density such that short-range ion–ion forces can be ignored, electrolytes obey the Boltzmann distribution:

$$\rho_B(r) = \sum_{\alpha=1}^{\nu} N_\alpha(r) z_\alpha e_0 = \sum_{\alpha=1}^{\nu} N_\alpha z_\alpha e_0 \exp[-z_\alpha e_0 \phi(r)/k_B T], \quad (2)$$

where $N_\alpha(r)$ is the local particle density of ions of type α (N_α are the values at infinity where the electric potential is zero), z_α the ionic valence, e_0 the electronic charge, k_B Boltzmann's constant, and T the temperature. Eqs. 1 and 2 comprise the the Poisson-Boltzmann equation.

Because they are nonlinear, Eqs. 1 and 2 are very difficult to solve analytically. Recently, we have developed a very efficient way to numerically solve the Poisson-Boltzmann equation for general cylindrically symmetric systems (Jordan et al., 1989). A finite difference equation was obtained by discretizing Eqs. 1 and 2 in a cylindrical coordinate system. The potential $\phi(r)$ is represented by $\phi(k, n)$ at points (k, n) on a regular cylindrical grid of mesh size δs in the radial direction and δz in the axial direction. The functions $\epsilon(r)$ and $N_\alpha(r)$ are determined in grid cells by $\epsilon(k, n)$ and $N_\alpha(k, n)$ which are constant inside each cell. The equations were solved by the conventional successive over-relaxation (SOR) method.

In the previous paper, the method was applied to a geometry in which the channel was a right circular cylinder and the external electrical source is either an ion on the cylinder axis or a transmembrane potential. For such a model channel, one may adjust the grid size so that grid points lie on the channel boundary. The advantage of doing so is that the dielectric constants and the concentrations in each cell are indeed constant. To apply the technique to the present problem in which much more

general shapes are considered, we need to take special care in treating those grid cells which include portions of the channel boundary, because $\epsilon(r)$ and N_α in these cells are discontinuous. To avoid this difficulty, we compute volume average values of the dielectric constant and the concentration in the boundary cells and thus estimate $\epsilon(k, n)$ and $N_\alpha(k, n)$. The fixed surface charge $\sigma(r)$ determines $q(k, n)$, the total charge in an annular cell with boundaries $(n - \frac{1}{2})\delta z$ to $(n + \frac{1}{2})\delta z$ in z-direction and $(k - \frac{1}{2})\delta s$ to $(k + \frac{1}{2})\delta s$ in r-direction. With these identifications, the electric potential can be evaluated as previously. We find that the convergence rate is the fastest when the relaxation factor, ω, is ~ 1.8.

We have checked the validity of our method by comparing our numerical calculation with the exact results of Gouy-Chapman theory. Fig. 2 shows the GC result and various numerical results with different grid sizes δs and δz. As expected, the smaller the grid sizes, the more accurate the numerical results. As long as the regions of major interest are well away from the charge sources, the numerical results are very close to the true values even for rather large grid sizes. For instance, if $\delta s = 0.6$ Å, $\delta z = 1.0$ Å and $I = 0.5$ M, the calculated value of the potential at 3.0 Å away from the source differs from the exact value only by 1.6%. More than 4.0 Å from the source, exact and numerical solutions are essentially indistinguishable.

GC theory, as augmented to include the influence of Stern layer, is valid at ionic strengths far larger than would be expected given the proviso on Eq. 2, that it is in principle only applicable at densities low enough that short range ion–ion forces can be ignored (McLaughlin, 1989). Our model is effectively an elaboration of the GC theory of surface charges to general geometries and surface charge distributions. Ionic strengths as high as 3.5 M are considered; at these concentrations ion–ion separations are <10 Å. Both theory (Carnie and Torrie, 1984) and experiment (McLaughlin et al., 1983) indicate that at high ionic strengths GC theory accounts for experimental observation roughly as well as more sophisticated statistical mechanical theories, although it is a less reliable tool when divalent ions are considered. We presume that our modified GC approach will be similarly successful.

RESULTS AND DISCUSSION

Conductance data

Recently, experiments (Green et al., 1987*a*) have described measurements of the concentration dependence of the conductance of single BTX-activated Na channels in planar lipid bilayers. The experimental data can be correlated using a slightly modified Michaelis-Menten

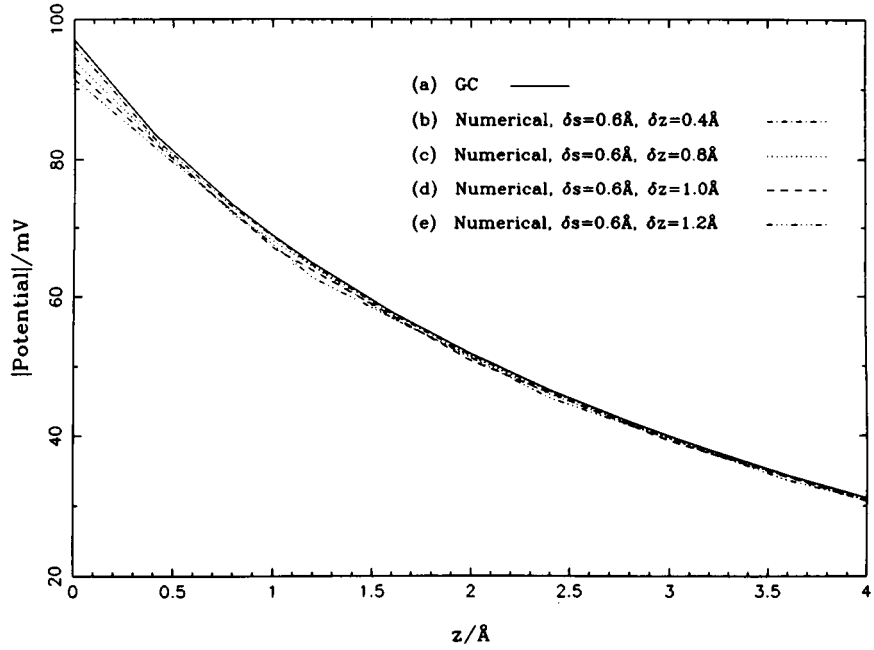

FIGURE 2 Comparison of GC and numerical results. The electrical potential as a function of the distance from the water–membrane interface. The solid line (*a*) is the exact GC result with the surface charge density $\sigma = e_0/60$ Å^2, and $I = 0.5$ M. The various dashed lines (*b to e*) are numerical results calculated with different grid spacing δs and δz.

expression:

$$g = \frac{g_\infty}{1 + K/[Na^+]_l} \tag{3}$$

where g is the conductance and $[Na^+]_l$ is the local concentration near the constricted region of Fig. 1; g_∞ and K are two parameters. As is well known, Eq. 3 is the result of a kinetic model which presumes only one ion may occupy the channel at any time. Although the Na channel is not a single-ion-occupancy channel (Garber, 1988), the modified Michaelis-Menten formula is a good approximation, particularly at low ionic strength. If there are negative surface charges near the constriction entrances, the local $[Na^+]_l$ is increased according to

$$[Na^+]_l = [Na^+] \exp(-e_0\phi_s/k_BT), \tag{4}$$

where ϕ_s is the electrical potential in the region of the entrance to the constriction, T is temperature, e_0 is electronic charge, and k_B is Boltzmann's constant. ϕ_s has been previously calculated in terms of Gouy-Chapman (GC) theory (McLaughlin, 1977, 1989),

$$\phi_s = \frac{2k_BT}{e_0} \operatorname{arcsinh}(\sigma/\sqrt{2\epsilon k_BT[Na^+]/\pi}), \tag{5}$$

where σ is an effective surface charge density and ϵ is the dielectric constant of the solution. Eqs. 3–5 were then used to interpret conductance-concentration data. By adjusting K, g_∞ and σ, one obtains an optimal fit to the experimental results.

Using the GC theory to calculate ϕ_s, one can correlate the experimental results; it is, however, by no means a good model to deal with this problem. First, the GC model presumes the potential arises from an infinite plane of charge at the membrane–electrolyte interface, but in a real channel the charges are only at the entrance. Whereas the electrical field at the interface depends only on the local charge distribution according to Coulomb's law, the electrical potential is determined by the charge distribution and geometry throughout all space. Hence, application of the GC theory to this problem cannot be correct. Second, according to the GC theory, as bulk $[Na^+] \to 0$, the local $[Na^+]$ at the membrane–electrolyte interface approaches a limit, $2\sigma^2\pi/(\epsilon k_BT)$. As a result, the low concentration conductance is predicted to approach a finite value. This is clearly wrong because, unlike an infinite plane of charge, a local charge leads to a finite potential in the vestibule as bulk electrolyte concentration $\to 0$. Thus, in the limit of $[Na^+] \to 0$, the local $[Na^+]$ in the vestibule must also approach zero. Our theoretical results indicate that the conductance falls off to zero very rapidly as $[Na^+]$ goes to zero.

We now present our method for correlating the experimental data. The geometrical model shown in Fig. 1 is used to describe a real sodium channel. As illustrated, a single electronic charge is spread around the entrance of the channel such that the surface charge density is cylindrically symmetric and no greater than $e_0/60$ Å^2. The dielectric constant of the pore is taken to be 80, that of bulk water. The mesh sizes of the grid δs and δz are 0.5 and 1.0 Å, respectively. The potential is then calculated by numerically solving the Poisson-Boltzmann equation. We choose the potential at site z_e (the constriction entrance, Fig. 1) as ϕ_s for Eq. 4. Our rationale for choosing this location is that it is the entrance to a single file region at which the ion completes its transition from bulk hydration to single file solvation. The $g - [Na^+]$ relation becomes:

$$g = \frac{g_\infty}{1 + K/\{[Na^+] \exp(-e_0\phi_s/k_BT)\}}. \tag{6}$$

Because ϕ_s is determined for a specific channel and surface charge density, there are only two remaining adjustable parameters, g_∞ and K. We use the linear least squares method to determine the parameters which provide the best fit of Eq. 6 to the experimental data.

Fig. 3 illustrates our correlation of the data of Green et al. (1987*a*). We have used the geometry: $L = 20$ Å, $R_v = 15$ Å, $a_0 = 3$ Å, $W = 20$ Å and the surface charge density $\sigma = 0.015e_0/$Å^2. It should be pointed out that this set of parameters is not the absolute best, one may further adjust L, R_v, and σ to obtain a somewhat better fit. Increasing W or decreasing a_0 to 2.5 Å has no effect on the results. It is essential that channel have the funnel shape and that the charges be near the constriction entrance. We have tried other geometries with charges located as shown in Fig. 4, none of them can correlate the data. This is because for all these geometries the potential at the entrance is far too low. For funnel-shaped channels with charges near the constriction, because of their narrow entrance, the field lines are concentrated and the potential at the entrance can be very high. Another point immediately apparent from Fig. 3 is that the conductance at low $[Na^+]$ decreases rapidly to zero, quite unlike the prediction of the GC theory.

For this geometry, with $\delta z = 1$ Å, $\delta r = 0.5$ Å, and $n = 100$, $k = 90$, about 6.5 min of CPU on a VAX 8650 are required for convergence for $I = 0.1$ M and 11 min for $I = 0.01$ M. The reduction to cylindrical symmetry permits efficient investigation of a variety of possible pore mouth geometries and surface charge distributions even at very low ionic strengths. We would be glad to make the program available to other investigators.

The sharp conductance drop occurs because Na^+ concentration at the constriction entrance, while always greater than in the bulk solution, falls off rapidly as bulk $[Na^+]$ decreases. Fig. 5 illustrates how local $[Na^+]$ at the constriction entrance depends on bulk electrolyte concen-

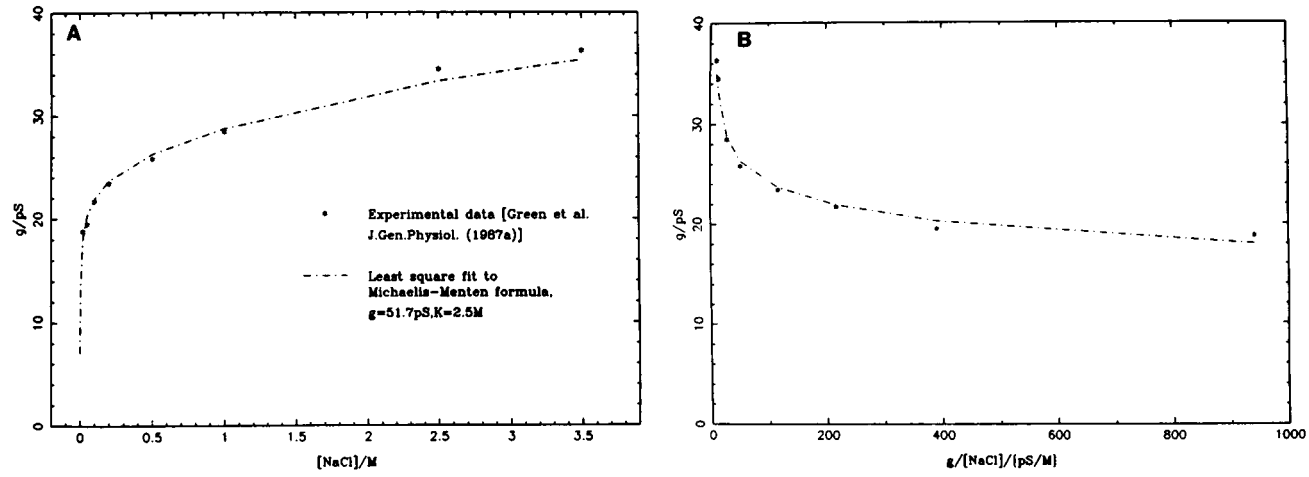

FIGURE 3 (*A*) The single-channel conductance, g, of Na channel as a function of NaCl concentration. The points denote the experimental data obtained by Green et al. (1987*a*). The curve is a fit of Eq. 6 to the data: g_∞ = 51.7 pS, K = 2.5 M. (*B*) Eadie-Hofstee plot of the data in *A*.

tration. We contrast the predictions of GC theory, for $\sigma = e_0/200$ Å^2, and our vestibule charge model. In GC theory, $[Na^+]$ at z_e is essentially a linear function of bulk $[Na^+]$. For a finite vestibule charge the local $[Na^+]$ is a linear function of bulk $[Na^+]$ over a fairly wide concentration range but it then falls off abruptly. For the model considered, the break occurs as the concentration drops from 0.2 to 0.1 M; here the Debye length increases from 6 to 10 Å. With the given channel geometry, the diffuse vestibule charges are ~5 Å from the point z_e. Thus, as the electrolyte concentration decreases further the potential at the constriction entrance is influenced by the absence of surface charge in the further regions of the vestibule. The potential still becomes increasingly negative, but it cannot change rapidly enough to maintain a high local cation concentration. It no longer approaches $-\infty$ as bulk

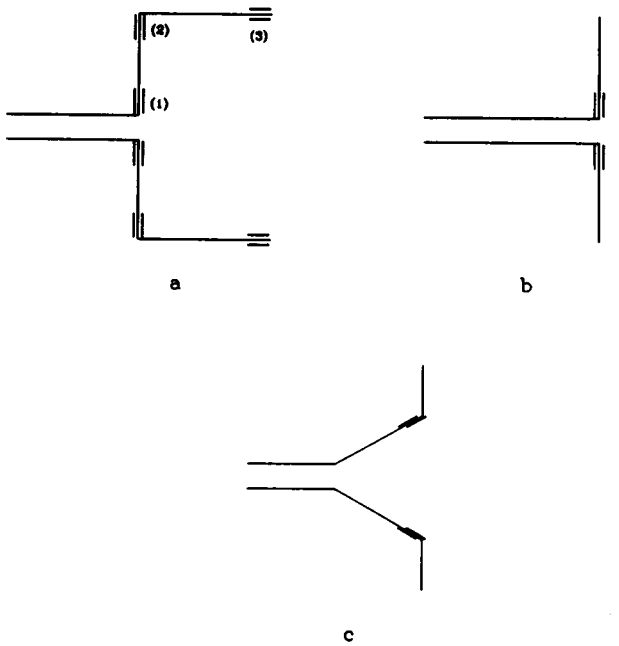

FIGURE 4 A schematic drawing illustrating other vestibule geometries considered. Here only half of the channel is drawn. In case *a*, three different charge locations were tested in our calculations. In *b* and *c*, the vestibule charges are located near the constriction entrance.

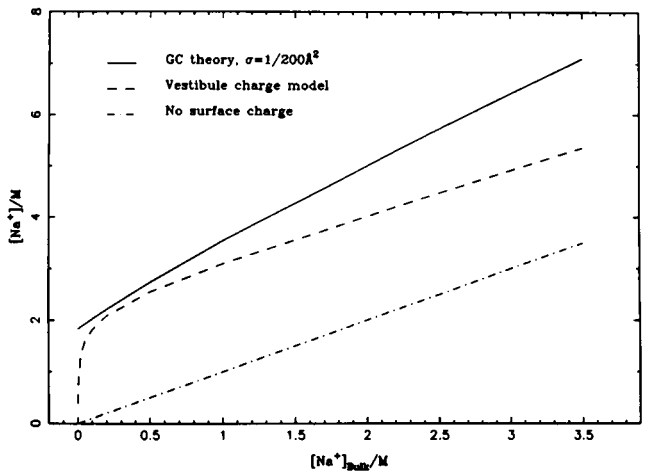

FIGURE 5 Local $[Na^+]$ at the constriction entrance as a function of bulk $[Na^+]$ for contrasting surface charge densities and models: GC theory (infinite plane of surface charge) with $\sigma = e_0/200$ Å^2; the vestibule charge model presented in the text; no surface charge. A low σ value is used in the GC calculation so that the local concentrations are comparable to those calculated from the vestibule charge model.

electrolyte concentration drops to zero; thus local [Na^+] must fall off to zero.

If one adds impermeant monovalent or divalent cations to the aqueous phases, the conductance decreases because of the screening of negative charges by these cations. Green et al. (1987*a*) measured the effects of two impermeant ions, Ba^{++} and TEA^+, on the conductance of the Na channel and correlated their results with the GC theory. We calculated the conductances by using our Na channel model and Eq. 6. The results are summarized in Table 1, demonstrating that the simple vestibule charge model is also a good correlational tool for conductance measurements in mixed electrolytes, without the further assumption that either TEA^+ or Ba^{++} necessarily act as blockers.

The dielectric constant of the pore, as mentioned earlier, could be much smaller than that of bulk water. We have tried other values for the pore dielectric constant and found that the pore entrance potentials are not very sensitive to them. For instance, if the pore dielectric constant is taken as 40, the potential ϕ_s at $I = 0.02$ M differs only by 3 mV from the potential calculated assuming a pore dielectric constant of 80. As the ionic strength, I, increases, the differences become smaller and at $I = 3.5$ M, there is virtually no difference. If the pore dielectric constant is 10, there is a potential difference of 6 mV at $I = 0.02$ M and no difference at $I = 3.5$ M. Such potential differences will cause only minor changes in fitting parameters g_∞ and K. As for the number of surface charges in the mouth, we have found that there is less flexibility for the choice of vestibule charges. To increase the surface charge, one spreads charge over wider area while keeping surface charge density constant. This will raise the pore potential considerably at low ionic strengths and cause no change at high ionic strengths. The results more closely resemble those of GC theory than when there is only a single charge; the fall off illustrated in Fig. 5 is less abrupt and shifted to somewhat lower concentrations. We have considered a few such models. For instance, if the vestibule charge is $4e_0$ and the charge density is the same, $\approx 0.015 e_0/Å^2$, but still localized to the vicinity of the constriction, the charge is spread out over a considerably greater region of the funnel. Here the potential is increased by 20 mV at $I = 0.02$ M and not at all at $I = 3.5$ M; the conductance data can still be correlated (but less well) on the basis of this assumption, although the fitting parameters are unreasonably large. As long as there is a single charge located in the vicinity of the constriction, we can always account for the experimental data. Even with the extra charge, the basic consequence of the limited charge model holds. The channel conductance is predicted to drop off precipitously as [Na^+] $\rightarrow$ 0; the concentration at which this drop off takes place does not change significantly as the total charge in the vestibule is increased from e_0 to $4e_0$. The extra charge is relatively far from the constriction entrance and has much less influence on the conduction process.

TABLE 1 Comparison of calculated and measured conductances for mixed electrolytes

Solution	ϕ_s	g(exp)*	g(calculated)
	mV	*pS*	*pS*
0.005M Ba^{++} + 0.02M Na^+ + 0.03M Cl^-	−63.6	5.4	4.6
0.02M Na^+ + 0.08M TEA^+ + 0.1M Cl^-	−74.5	8.2	6.63
0.05M Na^+ + 0.05M TEA^+ + 0.1M Cl^-	−74.5	13.5	13.9

*Data from Green et al. (1987*b*).

It is apparent that our model of the Na channel vestibule permits excellent correlation of the conductance measurements over a wide range of [Na^+], from 0.02 to 3.5 M. The model is also totally consistent with the mixed electrolyte measurements. Fig. 3, *A* and *B*, provide sensitive tests of the model since each emphasizes errors in different concentration domains, the direct correlation (Fig. 3 *A*) at high [Na^+] and the Eadie-Hofstee plot (Fig. 3 *B*) at low [Na^+]. The data of Table 1 provide further corroboration of the model in the critical, low–electrolyte concentration domain.

The parameters of the model, $g_\infty = 51.7$ pS and $K = 2.5$ M, are not unreasonable values for the limiting conductance and binding constant, given that the channel is treated as if it could only sustain single occupancy. Other single-file channels, such as gramicidin (which also may be multiply occupied), have $g_\infty = 14.6$ pS (Finkelstein and Anderson, 1981) when the data are correlated on the basis of a single occupancy model. The Michaelis-Menten constant for sodium association at the channel entrance superficially suggests that [Na^+] must be $\approx$2.5 M to half saturate the binding site. However this is misleading because the influence of the negative vestibule surface is treated separately. Only in experiments at very high concentrations of nonpermeant, nonblocking electrolytes would such high Na^+ concentrations be required. For the model geometry used, with sodium as the only cation, half saturation occurs at [Na^+] $\approx$ 0.5 M, a physiologically reasonable value and one that is consistent with earlier correlations of Na channel conductance data for frog node and squid giant axon using unmodified Langmiur isotherms (Hille, 1975; Bengenisich and Cahalan, 1980; Spires, 1985; Yamamoto et al., 1985).

Toxin binding data

It is well known that two guanidinium toxins, tetrodotoxin (TTX) and saxitoxin (STX), are both potent and specific

inhibitors for the Na channel (Hille, 1984). Their behavior and mechanism of interaction with the channel have been the subject of intensive studies. Recently, Green et al. (1987*b*) and Ravindran and Moczydlowski (1989) have investigated toxin binding to Na channels in planar lipid bilayers as a function of $[Na^+]$. They conclude that there is a net negative surface charge in the vicinity of the toxin-binding site. Their analyses were based on the Gouy-Chapman theory and competitive interaction between Na^+ and toxin binding at a single site.

The relationship between the toxin binding and $[Na^+]$ can be described as following (Green et al., 1987*b*):

$$K_D^{eff} = K_D\,(1 + [Na^+]_l/K_{Na}), \tag{7}$$

where $K_D^{eff} = k_d^{eff}/k_b^{eff}$, $K_D = k_d/k_b$ and $K_{Na} = k_{-Na}/k_{Na}$; k_b and k_{Na} are the binding constants for toxin and Na^+, respectively, k_d and k_{-Na} are dissociation constants, k_b^{eff} and k_d^{eff} are corresponding observed values. Because k_d should not depend on $[Na^+]$, the observed binding constant is

$$k_b^{eff} = \frac{k_b^0 \exp(-ze_0\phi_s/k_BT)}{1 + [Na^+]\exp(-e_0\phi_s/k_BT)/K_{Na}}, \tag{8}$$

where we have included the effect of electrical potential on both the toxin binding constant and the local Na^+ concentration, k_b^0 is the binding constant at $\phi_s = 0$, and z is the valence of the toxin.

Similarly to their handling of the conductance data, Green et al. (1987*b*) and Ravindran and Moczydlowski (1989) used Eq. 5 to calculate ϕ_s and correlate their toxin data with Eq. 8. However, there is once again a problem arising in application of the GC theory. As pointed out earlier, as bulk $[Na^+] \rightarrow 0$, the product of $[Na^+]$ and $\exp(-e_0\phi_s/k_BT)$ reaches a finite limit. Thus, according to Eq. 8 the observed binding constant, k_b^{eff}, is divergent in the low $[Na^+]$ limit. This problem can be avoided by using our Na channel model, because there is only a localized surface change at the mouth, the pore potential is finite as $[Na^+]$ goes to zero, not infinite as is the GC result. It is still a matter of controversy as to whether the toxin binds by occlusion (Green et al., 1987*b*). However, as both conductance and toxin binding appear to be influenced by similar surface potentials, it is reasonable to consider a model with the toxin binding site in the channel mouth.

To be consistent with our treatment of the conductance data, we use the same geometry and charge distribution to correlate Eq. 8 with the toxin binding data. The best fit is found if toxin binding and competition with Na^+ takes place at z_b, ~5–6 Å away from the site z_c, where ions enter the single-file region of the channel. If blocking is due to occlusion, it is quite possible that this reflects the size of the toxins which cannot get any closer to the entrance of the channel. Fig. 6 shows our correlation of the experimental results (Green et al., 1987*b*; Ravindran and Moczydlowski, 1989).

It is again clear that the simple vestibule model adequately accounts for the experimental observations for both mono- and divalent blockers. Of necessity the equilibrium constant for Na binding is independent of blocker valency; it does depend slightly on whether the channel is reconstituted from canine heart or brain. The rate constants for blocker binding, k_b^0, differ slightly from one another and are also slightly preparation dependent. More notably, for the canine brain preparation the equi-

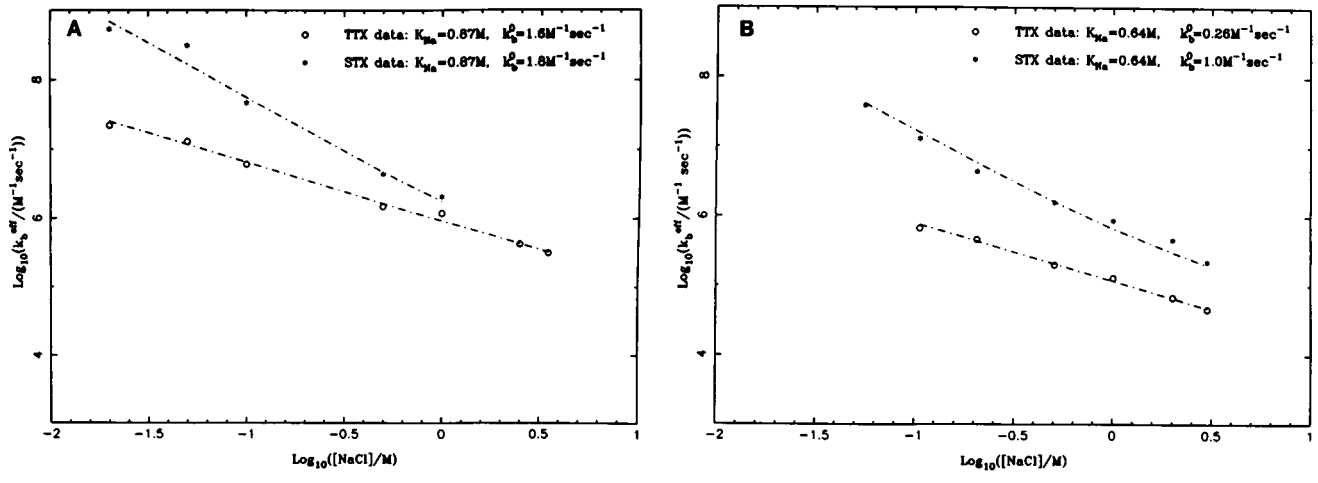

FIGURE 6 Toxin binding coefficient, k_b^{eff}, as a function of NaCl concentration. Experimental values are represented by (o) and (*) for TTX and STX, respectively; the fits of Eq. 8 to the data are shown by the dashed lines. (*A*) The data taken from Ravindran and Moczydlowski (1989). (*B*) The data from Green et al. (1987); the Na^+ affinity constants which best correlate the data are 0.87 and 0.64 M, respectively.

librium constant for Na binding in the toxin competition region is less than the Michaelis-Menten K of Eq. 6. It should be further noted that the larger affinity at the toxin binding site is not a reflection of the fact that the influence of the vestibule surface charge is accounted for separately. As already indicated, the entrance site is half saturated at $[Na^+] \approx 0.5$ M; including the effect of the vestibule charges, the blocking site half-saturates at $[Na^+] \approx 0.05$ M.

That $K_{Na} < K$ is not unreasonable, even though K, for a single site model, is interpreted as $(k_{off} + k_{tr})/k_{on}$, where k_{on} is the rate of association in the vicinity of z_e, k_{off} the corresponding rate of dissociation of k_{tr} the rate at which the ion translocates further into the single file region of the channel. Thus the Michaelis-Menten constant describing the kinetics of ion entry into the narrow part of the channel is greater than the equilibrium constant K_{Na}. Why might this be so? If we assume competition occurs near the constriction entrance, two speculations are immediately plausible. One, consistent with use of the single occupancy model, is that once the ion arrives at the entrance to the constriction, it moves rapidly into the narrow part of the channel in which case $k_{tr} \gg k_{off}$ and the K of Eq. 6 is dominated by the rate k_{tr}. Alternatively, k_{tr} may be smaller than k_{off}. In this case the Michaelis-Menten constant is just the reciprocal of the binding constant for Na at the entrance to the single file region and the relative values of K and K_{Na} would indicate that binding of Na at the entrance is less favorable than association of Na in the region of the vestibule where the ion competes with the toxin. A possible rationalization for either interpretation is that in the vicinity of z_b, an ion on the axis is at least 5.5 Å from the walls of our model vestibule. At this distance it can maintain its full first hydration shell. In moving to the constriction entrance it must shed a substantial number of its waters of hydration and resolvate to the protein itself. This process could well involve an increase in free energy; if this is so the affinity at z_b would be greater than that at z_e. The inequality $K_{Na} < K$ could equally well reflect the relationship $k_{off} < k_{tr}$ because the off rate, k_{off}, requires rearrangement and resolvation to water, a process that might well be slow with respect to further migration into the channel, governed by k_{tr}. In the absence of structural information that would permit molecular modeling of the toxin-Na^+ competition, these suggestions are of course highly speculative.

SUMMARY

We have reanalyzed conductance and toxin block data for Na channels reconstituted from different canine preparations. We find that the data can be well accomodated by a model channel geometry in which there are funnel shaped charged vestibules separated by a long, narrow transmembrane channel. We find that, as long as there is at least a single vestibule charge located near the entrance to the channel constriction, large vestibule potentials are generated. Somewhat surprisingly, Na binding affinity appears to be greater at the site of competition with toxin than at the entrance to the constriction itself. Unlike correlations based upon Gouy-Chapman theory, we show that as Na concentration is decreased, the channel conductance falls to zero. Furthermore, we show that the apparent binding constant for toxin binding should approach a limit as $[Na^+]$ decreases, not increase indefinitely.

The authors wish to thank C. Miller, R. MacKinnon, and D. Cherbavez for useful discussions.

This work is supported by the National Institutes of Health through grant GM-28643.

Received for publication 22 September 1989 and in final form 18 December 1989.

REFERENCES

Begenisich, T. B. 1987. Molecular properties of ion permeation through sodium channels. *Annu. Rev. Biophys. Biophys. Chem.* 16:247–263.

Begenisich, T. B., and M. D. Cahalan. 1980. Sodium channel permeation in squid axons. II. Non-independence and current-voltage relations. *J. Physiol. (Lond.).* 307:243–257.

Carnie, S. L., and G. M. Torrie. 1984. The statistical mechanics of the electrical double layer. *Adv. Chem. Phys.* 56:141–253.

Dani, J. A. 1986. Ion-channel entrances influence permeation, net charge, size, shape, and binding considerations. *Biophys. J.* 49:607–618.

Finkelstein, A., and O. S. Anderson. 1981. The gramicidin A channel: a review of its permeability characteristics with special reference to the single-file aspect of transport. *J. Membr. Biol.* 59:155–171.

Garber, S. S. 1988. Symmetry and asymmetry of permeation through toxin-modified Na^+ channels. *Biophys. J.* 54:767–776.

Green, W. N., L. B. Weiss, and O. S. Andersen, 1987*a*. Batrachotoxin-modified sodium channels in planar lipid bilayers. Ion permeation and block. *J. Gen. Physiol.* 89:841–872.

Green, W. N., L. B. Weiss, and O. S. Andersen. 1987*b*. Batrachotoxin-modified sodium channels in planar lipid bilayers. Characterization of saxitoxin- and tetrodotoxin-induced channel closures. *J. Gen. Physiol.* 89:873–903.

Hess, P., and P. W. Tsien. 1984. Mechanism of ion permeation through calcium channels. Nature (*Lond.*). 309:453–456.

Hille, B. 1975. Ionic selectivity, saturation, and block in sodium channels. A four-barrier model. *J. Gen. Physiol.* 66:535–560.

Hille, B. 1984. Ionic Channels of Excitable Membranes. Sinauer Associates, Inc., Sunderland, MD.

Hille, B., and E. Schwartz. 1978. Potassium channels as multi-ion single-file pores. *J. Gen. Physiol.* 72:409–442.

Jordan, P. C. 1982. Electrostatic modeling of ion pores. Energy barriers and electric field profiles. *Biophys. J.* 39:157–164.

Jordan, P. C. 1983. Electrostatic modeling of ion pores. II. Effects attributable to the membrane dipole potential. *Biophys. J.* 41:189–195.

Jordan, P. C. 1984. The effect of pore structure on energy barriers and applied voltage profiles. I. Symmetrical channels. *Biophys. J.* 45:1091–1100.

Jordan, P. C. 1986. Ion channel electrostatics and the shape of channel proteins. *In* Ion Channel Reconstitution. C. Miller, (editor). Plenum Publishing Corp., New York. 37–55.

Jordan, P. C. 1987. How pore mouth charge distribution alter the permeability of transmembrane ionic channels. *Biophys. J.* 51:297–311.

Jordan, P. C., R. J. Bacquet, J. A. McCammon, and P. Tran. 1989. How electrolyte shielding influences the electrical potential in transmembrane ion channels. *Biophys. J.* 55:1041–1052.

Kistler, J., R. M. Stroud, M. W. Klymkowsky, R. A. Lalancette, and R. H. Fairclough. 1982. Structure and function of an acetylcholine receptor. *Biophys. J.* 37:371–383.

Levitt, D. G. 1978. Electrostatic calculations for an ion channel. I. Energy and potential profiles and interaction between ions. *Biophys. J.* 22:209–219.

McLaughlin, S. 1977. Electrostatic potentials at membrane-solution interfaces. *Curr. Top. Membr. Transp.* 9:71–144.

McLaughlin, S. 1989. The electrostatic properties of membranes. *Annu. Rev. Biophys. Biophys. Chem.* 18:113–136.

McLaughlin, A., W.-K. Eng, G. Vai, T. Wilson, and S. McLaughlin. 1983. Dimethonium, a divalent cation that exerts only a screening effect on the electrostatic potential adjacent to negatively charged phospholipid bilayer membranes. *J. Membr. Biol.* 76:183–193.

Miller, C., and S. S. Garber. 1988. Sodium channels in lipid bilayers: have we learned anything yet? *Curr. Top. Membr. Transp.* 33:309–327.

Parsigian, V. A. 1969. Energy of an ion acrossing a low dielectric membrane: solution to four relevant electrostatic problems. *Nature (Lond.).* 221:844–846.

Ravindran, A., and E. Moczydlowski. 1989. Influence of negative surface charge on toxin binding to canine heart Na channels in planar bilayers. *Biophys. J.* 55:359–365.

Spires, S. 1985. Sodium channel saturation and alteration of current kinetics by several permeant ions. *Biophys. J.* 47:437a. (Abstr.)

Yamamoto, D., J. Z. Yeh, and T. Narahashi. 1985. Interactions of permeant cations with sodium channels of squid axon membranes. *Biophys. J.* 48:361–368.